electroretinogram in case of polypoidal choroidopathy treated with photodynapic therapy. Jpn J Ophthalmol. 2010; 54: 509-511.

4. **Machida S,** Takahashi T, Gotoh N, Yoshimura N, Fujiwara T, Kurosaka D. Monozygotic twins of polypoidal choroidal vasuculopathy. Clin Ophthalmol. 2010; 4: 793-800.

5. **Machida S,** Tamada K, Oikawa T, Gotoh Y, Nishimura T, Yokoyama D, Kurosaka D. Comparison of photopic negative response between full-field and focal electroretinograms in detecting glaucomatous eyes. J Ophthalmol. 2011.

学会発表

1. 町田繁樹. PhNR と網膜内層 Imaging. 第 114 回日本眼科学会総会, 2011 年 4 月 15 日,名古屋.

2. Machida S, et al. Sensitivity and specificity of photopic negative response of focal electoretinogram to discriminate glaucomatous eyes. ARVO, 2010 年 5 月 4 日, Fort Lauderdale, USA.

3. Machida S, et al. Clinical application of the focal photopic negative response to patients with open angle glaucoma. ISCEV, 2010 年 11 月 7 日, Fremantle, Australia.

H. 知的財産権の出願・登録状況

1. 特許取得
   なし
2. 実用新案登録
   なし
3. その他
   なし

Ⅲ. 研究成果の刊行に関する一覧表

研究成果の刊行に関する一覧表

雑 誌

発 表 者 氏 名	論 文 タ イ ト ル	発 表 誌 名	巻 号	ページ	出版年
Akahori M, Tsunoda K, Miyake Y, Fukuda Y, Ishiura H, Tsuji S, Usui T, Hatase T, Nakamura M, Ohde H, Itabashi T, Okamoto H, Takada Y, Iwata T	Dominant mutations in RP1L1 are responsible for occult macular dystrophy	Am J Hum Genet	87(3)	424-429	2010
Kazato Y, Shibata N, Hanazono G, Suzuki W, Tanifuji M, Tsunoda K	Snapshot Imaging of Photoreceptor Bleaching in Macaque and Human Retinas	Jpn J Ophthalmol	54(4)	349-356	2010
Fujinami, K, Akahori M, Fukui M, Tsunoda K, Iwata T, Miyake Y	Stargardt Disease with Preserved Vision: identification of a novel mutation in ATP-binding cassette transporter gene	Acta Ophthalmologica		Epub ahead of print	2010
Fujinami K, Kazushige Tsunoda K, Hanazono G, Shinoda K, Ohde H, Miyake Y	Fundus Autofluorescence in Autosomal Dominant Occult Macular Dystrophy	Arch Ophthalmol	129	597-602	2011
Fujinami K, Tsunoda K, Nakamura M, Oguchi Y, Miyake Y	Oguchi's Disease with Unusual Findings Associated with a Heterozygous Mutation in SAG Gene	Arch Ophthalmol		in press	
Tsunoda K, Fujinami K, Miyake Y	Selective abnormality of the cone outer segment tip line in acute zonal occult outer retinopathy as observed by Fourier domain optical coherence tomography	Arch Ophthalmol		in press	
Hanazono G, Ohde H, Shinoda K, Tsunoda K, Tsubota K, Miyake Y	Pattern- reversal visual-evoked potential in patients with occult macular dystrophy	Clinical Ophthalmology	10(4)	1515 -1520	2010
Omori Y, Chaya T, Katoh K, Kajimura N, Sato S, Muraoka K, Ueno S, Koyasu T, Kondo M, Furukawa T	Negative regulation of ciliary length by ciliary male germ cell-associated kinase (Mak) is required for retinal photoreceptor survival	Proc Natl Acad Sci U S A	107	22671 -22676	2010
Kondo M, Mokuno K, Uemura A, Kachi S, Nakamura M, Kondo A, Terasaki H	Paraneoplastic retinopathy associated with retroperitoneal liposarcoma	Clin Ophthalmol	4	243-245	2010
Nakamura M, Sanuki R, Yasuma TR, Onishi A, Nishiguchi KM, Koike C, Kadowaki M, Kondo M, Miyake Y, Furukawa T	TRPM1 mutations are associated with the complete form of congenital stationary night blindness	Mol Vis	16	425-437	2010

Koike C, Obara T, Uriu Y, Numata T, Sanuki R, Miyata K, Koyasu T, Ueno S, Funabiki K, Tani A, Ueda H, Kondo M, Mori Y, Tachibana M, Furukawa T	TRPM1 is a component of the retinal ON bipolar cell transduction channel in the mGluR6 cascade	Proc Natl Acad Sci U S A	107	332-337	2010
近藤峰生	網膜・視神経疾患動物モデルの網膜電図解析	日眼会誌	114	248-278	2010
Gekeler F, Kobuch K, Blatsios G, Zrenner E, Shinoda K	Repeated transchoroidal implantation and explantation of compound subretinal prostheses: an exploratory study in rabbits	Jpn J Ophthalmol	54 (5)	467-475	2010
Hanazono G, Ohde H, Shinoda K, Tsunoda K, Tsubota K, Miyake Y	Pattern-reversal visual evoked potential in patients with occult macular dystrophy	Clin Ophthalmol	10 (4)	1515 -1520	2010
Matsumoto CS, Shinoda K, Nakatsuka K	High Correlation of Scotopic and Photopic ERG Components with Severity of Ocular Circulation Disturbances Following Central Retinal Artery Occlusion	Clin Ophthalmol	20 (5)	115-121	2011
Akahori M, Tsunoda K, Miyake Y, Fukuda Y, Ishiura H, Tsuji S, Hatase T, Nakamua M, Ohde H, Itabashi T, Okamoto H, Takada Y, Iwata T	Dominant mutations in *RP1L1* gene are responsible for occult macular dystrophy	The American Journal of Human Genetics	87	424-429	2010
Kuniyoshi K, Irifune M, Uno N, Nakao A, Shimomura Y	Oscillatory potentials with repeated- flash electroretinography	Jpn J Ophthalmol	54	32-35	2010
南里勇, 國吉一樹, 中尾彰, 他	比較的短期間に近視が進行した網膜色素線条の１例	眼臨紀	3	580-586	2010
Sugawara E, Machida S, Fujiwara T, Hayakawa M, Kurosaka D	Punctate inner choroidopathy occurring in mother and daughter	Jpn J Ophthalmol	54	505-507	2010
Yokoyama D, Machida S, Kondo M, Nishimura T, Terasaki H, Kurosaka D	Pharmacological dissection of multifocal electroretinograms of rabbits with Pro347L rhodopsin mutation	Jpn J Ophthalmol	54	458-466	2010
Nishimura T, Machida S, Tamada K, Kurosaka D	Depolarizing pattern of the focal macular electroretinogram in case of polypoidal choroidopathy treated with photodynapic therapy	Jpn J Ophthalmol	54	509-511	2010
Machida S, Takahashi T, Gotoh N, Yoshimura N, Fujiwara T, Kurosaka D	Monozygotic twins of polypoidal choroidal vasuculopathy	Clin Ophthalmol	4	793-800	2010
Machida S, Tamada K, Oikawa T, Gotoh Y, Nishimura T, Yokoyama D, Kurosaka D	Comparison of photopic negative response between full-field and focal electroretinograms in detecting glaucomatous eyes	J Ophthalmol			2011

Ⅳ. 研究成果の刊行物・別刷

REPORT

Dominant Mutations in *RP1L1* Are Responsible for Occult Macular Dystrophy

Masakazu Akahori,[1] Kazushige Tsunoda,[1] Yozo Miyake,[1,2] Yoko Fukuda,[3] Hiroyuki Ishiura,[3] Shoji Tsuji,[3] Tomoaki Usui,[4] Tetsuhisa Hatase,[4] Makoto Nakamura,[5] Hisao Ohde,[6] Takeshi Itabashi,[1] Haru Okamoto,[1] Yuichiro Takada,[1] and Takeshi Iwata[1,*]

Occult macular dystrophy (OMD) is an inherited macular dystrophy characterized by progressive loss of macular function but normal ophthalmoscopic appearance. Typical OMD is characterized by a central cone dysfunction leading to a loss of vision despite normal ophthalmoscopic appearance, normal fluorescein angiography, and normal full-field electroretinogram (ERGs), but the amplitudes of the focal macular ERGs and multifocal ERGs are significantly reduced at the central retina. Linkage analysis of two OMD families was performed by the SNP High Throughput Linkage analysis system (SNP HiTLink), localizing the disease locus to chromosome 8p22-p23. Among the 128 genes in the linkage region, 22 genes were expressed in the retina, and four candidate genes were selected. No mutations were found in the first three candidate genes, methionine sulfoxide reductase A (*MSRA*), GATA binding 4 (*GATA4*), and pericentriolar material 1 (*PCM1*). However, amino acid substitution of p.Arg45Trp in retinitis pigmentosa 1-like 1 (*RP1L1*) was found in three OMD families and p.Trp960Arg in a remaining OMD family. These two mutations were detected in all affected individuals but in none of the 876 controls. Immunohistochemistry of RP1L1 in the retina section of cynomolgus monkey revealed expression in the rod and cone photoreceptor, supporting a role of RP1L1 in the photoreceptors that, when disrupted by mutation, leads to OMD. Identification of *RP1L1* mutations as causative for OMD has potentially broader implications for understanding the differential cone photoreceptor functions in the fovea and the peripheral retina.

Occult macular dystrophy (OMD) is an autosomal-dominant form of inherited macular dystrophy characterized by progressive decrease of visual acuity due to macular dysfunction, which was first reported by Y.M. et al. in 1989.[1–3] The disorder was called "occult" because of the fact that the macular dysfunction of this disease is hidden by a normal fundus appearance. Typical OMD, as described by Y.M. et al., is characterized by central cone dysfunction and in some cases rod dysfunction, leading to a loss of vision despite normal ophthalmoscopic appearance, normal fluorescein angiography, and normal full-field electroretinograms (ERGs). However, the amplitudes of the focal macular ERGs and multifocal ERGs are significantly reduced, indicating dysfunction of the central retina.[1,2,4] OMD is known for its broad range of age at disease onset, from 6 to 81 yrs. Brockhurst et al. have reported age at onset of four out of eight OMD patients at over 65 yrs[5] and similar findings have also been observed in earlier cases.[1,2] The patient III-3 in family 1 did not notice any visual disturbance in her right eye even at the age of 81 yrs.

The four families shown in Figure 1 demonstrate dominant inheritance of the OMD phenotype. None of the patients had ocular diseases other than OMD, except senile cataract or diabetic retinopathy. Control family members were confirmed to be normal via a complete ophthalmic examination including focal macular ERGs or multifocal ERGs. For this study, the ethics review committees of the National Hospital Organization Tokyo Medical Center, the Niigata University Graduate School of Medical and Dental Sciences, and the Nagoya University Medical School approved the study, and written informed consent was obtained from both affected and unaffected subjects.

Linkage analysis of OMD families 1 and 2 was performed. Eighteen individuals from family 1 and eleven individuals from family 2 were genotyped by Affymetrix's Genome-Wide Human SNP array 6.0 in accordance with the manufacturer's instructions (Affymetrix, Santa Clara, CA). DNA samples from family 2 were subjected to whole-genome amplification with the use of REPLI-g (QIAGEN, Tokyo, Japan) prior to SNP genotyping. With SNP HiTLink[6] used as a pipeline, SNPs with a Hardy-Weinberg p value $>$ f 0.001, a call rate of 1, and a maximum confidence score $>$ 0.02 were used for the analysis. SNPs with the minor allele frequency of 0 in controls were eliminated from the analysis. Parametric multipoint linkage analysis (autosomal-dominant model with a setting of liability classes; age-dependent penetrance of 0.19, 0.55, and 0.91 for 0–20, 21–40, and $>$ 41 yrs old, respectively, and disease frequency of 0.000001) was performed with Allegro version 2,[7] intermarker distance from 80 kb to 120 kb with the use of SNP HiTLink. Because of the limitation of computational capacity, family 1 was divided into two branches (branch 1-1: descendants of II-1; branch

[1]National Institute of Sensory Organs, National Hospital Organization Tokyo Medical Center, 2-5-1 Higashigaoka, Meguro-ku, Tokyo 152-8902 Japan; [2]Aichi Medical University, 21 Yazakokarimata, Nagakute-cho, Aichi-gun, Aichi-ken, 489-1195 Japan; [3]Department of Neurology, Graduate School of Medicine, the University of Tokyo, 7-3-1, Hongo, Bunkyo-ku, Tokyo, 113-8655 Japan; [4]Division of Ophthalmology and Visual Science, Graduate School of Medical and Dental Sciences, Niigata University, Niigata, 757, Ichibancho, Asahimachidori, Niigata, 951-8510 Japan; [5]Nakamura Eye Clinic, 107-10, Kisei-cho, Nishi-ku, Nagoya, 452-0816 Japan; [6]Department of Ophthalmology, School of Medicine, Keio University, 35 Shinanomachi, Shinjuku-ku, Tokyo 160-8582, Japan
*Correspondence: iwatatakeshi@kankakuki.go.jp
DOI 10.1016/j.ajhg.2010.08.009.

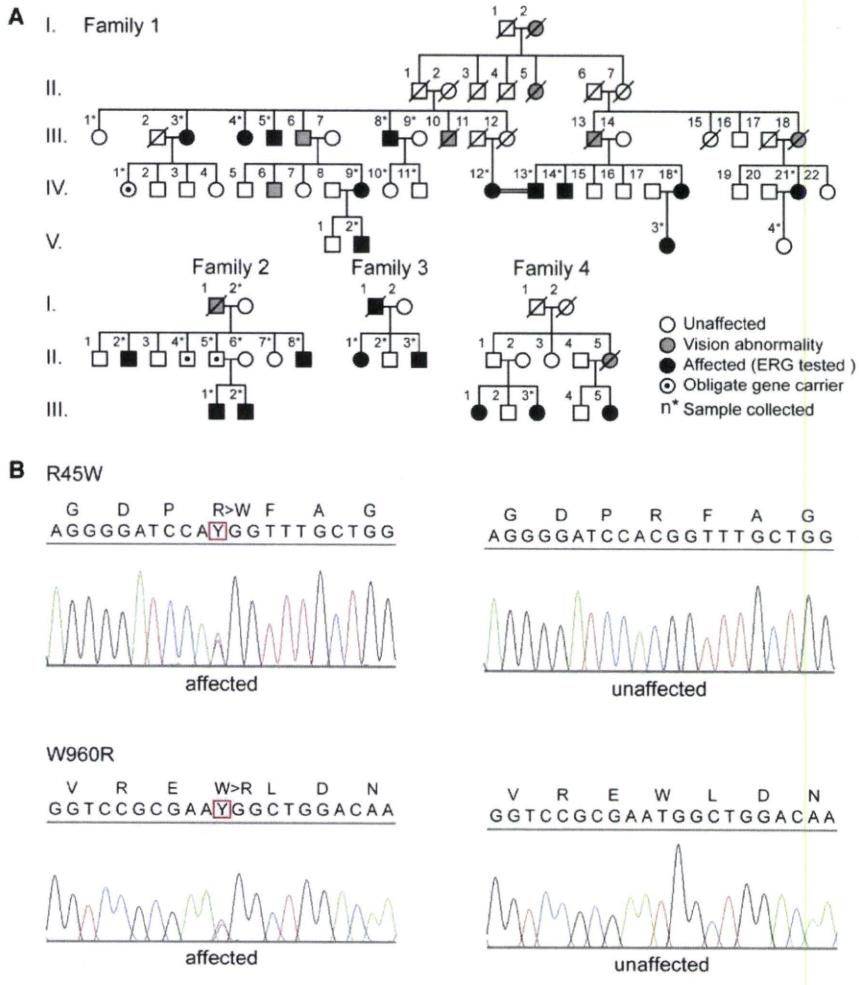

Figure 1. Autosomal OMD Families and DNA Sequencing of *RP1L1*

(A) The four families shown demonstrate dominant inheritance of the OMD phenotype. In all presented families, none of the patients had ocular diseases other than OMD, except senile cataract and diabetic retinopathy. Control family members were confirmed to be normal via a complete ophthalmic examination including focal macular ERGs or multifocal ERGs.

(B) DNA sequencing of both p.Arg45Trp and p.Trp960Arg mutations found in four independent families.

1-2: descendants of II-7) for multipoint linkage analysis. Haplotypes were reconstructed by Allegro.

The parametric linkage study of family 1 using SNP microarrays and SNP HiTLink mapped the disease locus to an approximately 10 Mb region of chromosome 8p22-p23 with a maximum LOD score of 3.77 (Figure 2). Parametric linkage analysis of affected individuals only produced similar results (Figure 3 and Figure S2 available online). A common haplotype between rs365309 and rs2632841 was shared by all of the affected individuals (Table 1). With the additional linkage study of family 2, the cumulative parametric multipoint LOD score rose to over 4 (Figure S1). A total of 128 known genes were found within the approximately 10 Mb linkage-associated region, containing 22 retina-expressed genes as candidates for mutational analyses. No mutations were found in the first three candidate genes, methionine sulfoxide reductase A (*MSRA*), GATA binding 4 (*GATA4*), and pericentriolar material 1 (*PCM1*). However, a c.362C>T (p.Arg45Trp) substitution in retinitis pigmentosa 1-like 1 (*RP1L1* [MIM 608581]) was found in all affected individuals in family 1. We further extended the mutational analysis of *RP1L1* to three other families with autosomal OMD, and we identified the p.Arg45Trp alteration in families 2 and 4 and a c.3107T>C (p.Trp960Arg) mutation in family 3 (Table 2). Additionally, known and unknown natural variants were found in *RP1L1*, as shown in Table S2. Unknown SNPs were submitted to the dbSNP database.

In these four families, all of the affected individuals carried one of the two mutations identified in this study, c.362C>T or c.3107T>C. We identified three apparently unaffected individuals carrying the p.Arg45Trp mutation, which suggest a reduced penetrance of the mutation or possibility a later onset of the disease for these individuals. Both mutations were absent in 1752 Japanese control chromosomes.

Immunohistochemistry of RP1L1 in the macula section of primate Cynomolgus monkeys (*Macaca fascicularis*) was performed. The eyes from a 6-yr-old normal male cynomolgus monkey were obtained from Tsukuba Primate Research Center, National Institute of Biomedical Innovation, Japan. All experimental procedures were approved by the Animal Welfare and Animal Care Committee of the National Institute of Biomedical Innovation, in compliance with guidelines of the Association for Research in Vision and Ophthalmology. Cynomolgus eyes were removed and immediately fixed overnight with 4% paraformaldehyde in 0.1 M phosphate buffer, pH 7.4. After washing in PBS, eyes were cryoprotected in the gradient sucrose dissolved in PBS and embedded into optimal cutting temperature (OCT) compound (Tissue Tek, Miles, IL, USA). Frozen retinal sections cut at 8 μm thickness with cryostat were incubated at 4°C with a 1:500 dilution of human RP1L1 polyclonal antibody raised against the N terminus of human RP1L1 (Santa Cruz Biotechnology, Santa Cruz, CA, USA). Immunofluorescence was visualized with Alexa 568 goat anti-rabbit IgG (Invitrogen, Carlsbad, CA, USA), Alexa 488 PNA (Invitrogen) for detection of cone photoreceptor, and DAPI (Invitrogen) for nuclear staining. Fluorescence images were analyzed with a confocal laser

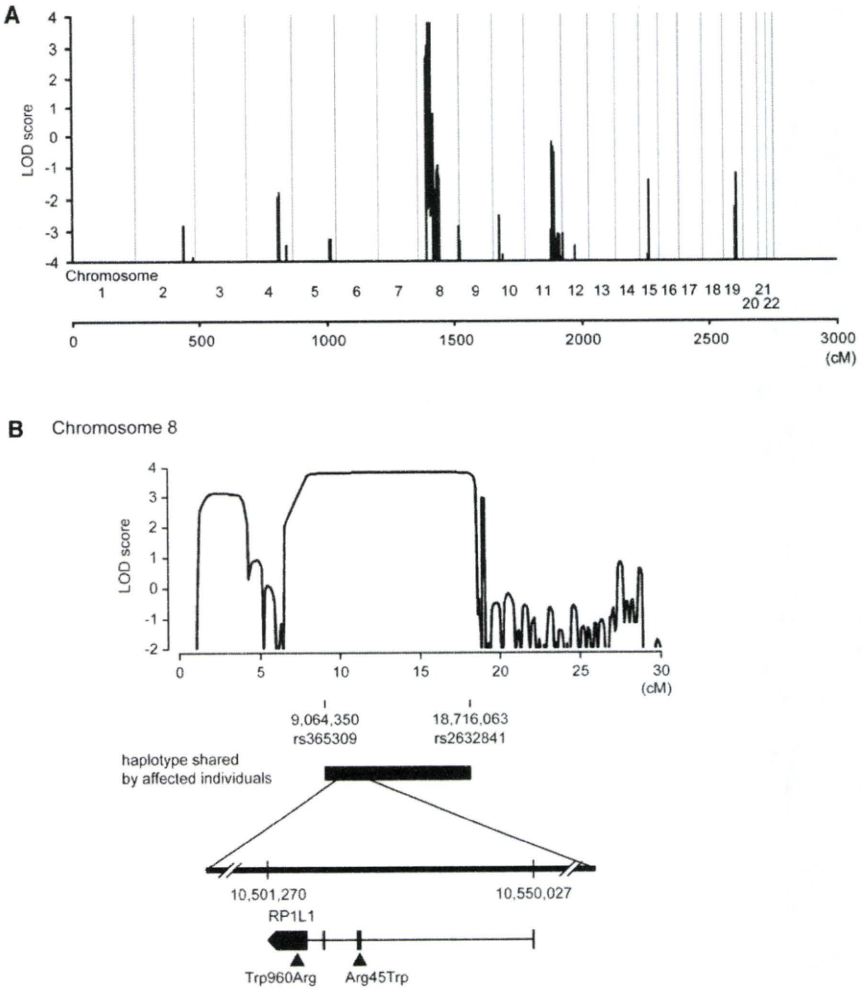

Figure 2. Linkage Analysis and Haplotype Analysis of Family 1

(A) Parametric multipoint linkage analysis of family 1. Horizontal axis indicates cumulative position (cM) from the short arm of chromosome 1. As a result of computational capacity, family 1 was divided into two branches for calculation of LOD scores. No other chromosomes except chromosome 8 yielded a positive LOD score.

(B) Parametric multipoint linkage analysis of family 1 and mutations in *RP1L1*. A maximum LOD score of 3.77 was obtained at 8p32.1-8p22. A haplotype bounded by rs365309 (physical position: 9,064,350 in the hg18 assembly of the UCSC Genome Browser) and rs2632841 (18,716,063) was shared by all affected individuals. Horizontal axis indicates the position (cM) on the short arm of chromosome 8. Vertical axis indicates the parametric multipoint LOD score. Mutations (p.Arg45Trp and p.Trp960Arg) are demonstrated.

microscope (Radiance 2000, Bio-Rad Laboratories, Hercules, CA, USA).

To our surprise, the immunohistochemistry of RP1L1 in the macula section of Cynomolgus monkeys revealed expression in retinal rod and cone photoreceptors by human RP1L1 antibody (Figure 3). This expression pattern is significantly different from the previous study of mouse RP1L1, in which RP1L1 was localized exclusively in axoneme of rods.[8] Furthermore, the human amino acid sequence is only 39% identical to that of the mouse, due to a lack of both polymorphic 16 amino acid repeats or a lack of the highly repetitive Glu-rich region, making mouse RP1L1 protein considerably shorter than the human protein, which may lead to different functional roles in the primate retina. Recent investigation of photoreceptor structure in OMD patients using advanced optical coherence tomography suggests that the predominant defect involves the cone photoreceptor.[9,10] Our optical coherence tomography observations also show loss of the cone outer segment tip and irregularity of the inner segment/outer segment junction in the center of the macula of all examined case individuals in family 1 (data not shown). Y.M. et al. have observed that not only cone but also rod sensitivity in the macula was abnormal in some of the older patients.[1,2] It is likely that the initial event may be macular cone specific but may later extend to rod abnormality. Further investigation of RP1L1 function is required in order to answer these clinical observations.

RP1L1 was originally cloned as a gene derived from common ancestor as retinitis pigmentosa 1 (*RP1* [MIM 180100]) on the same chromosome 8.[11,12] *RP1L1* shares 35% amino acid identity with *RP1*, a gene responsible for 5%–10% of autosomal-dominant retinitis pigmentosa (RP [MIM 268000]) worldwide.[13–15] When *RP1L1* was first identified, a number of attempts were made to identify mutations in *RP1L1* in various RP patients, with no success. The present study demonstrates that *RP1L1* mutation is responsible for OMD, but not for RP. Patients with RP carrying the most common RP1 alteration, p.Arg677X, exhibit night and peripheral vision disturbance beginning in the third decade of life. RP1 is found exclusively in the retina and is localized to both rods and cones. Rod-cone functional comparison in RP patients has indicated that rod sensitivity loss is at least 2 log units greater than cone sensitivity loss.[13] Thus phenotypic characteristics of RP caused by *RP1* mutations and those of OMD caused by *RP1L1* mutations perfectly agree with the different localizations of RP1 and RP1L1 in retina.

The outer segments of rod and cone photoreceptors are highly specialized cilia containing hundreds of disc membranes stacked in an orderly array along the photoreceptor axoneme. Previous studies have shown that RP1 is part of the axoneme and is required for this correct orientation and higher-order stacking of outer segment discs.[16] This is achieved by the interaction of RP1 with the

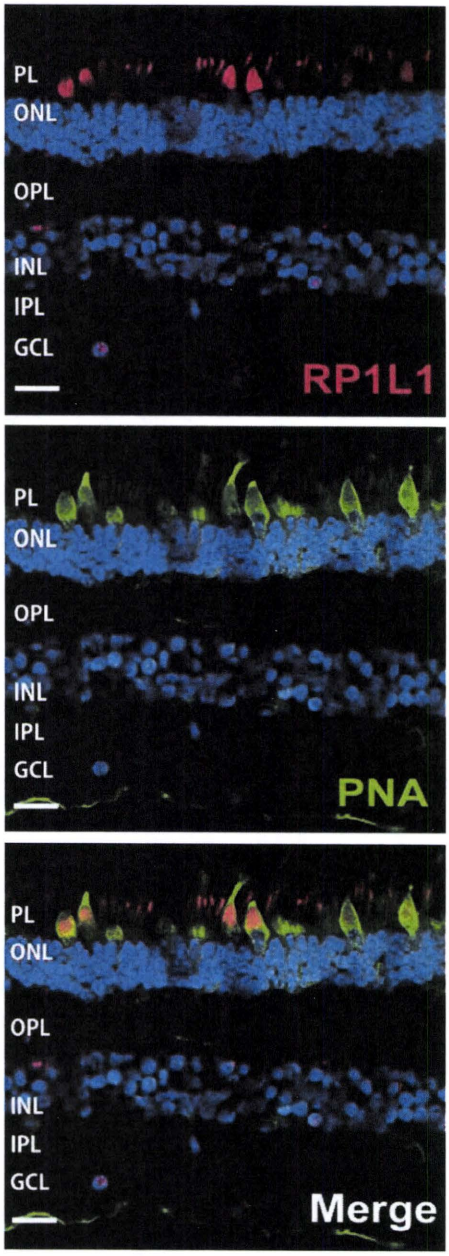

Figure 3. Immunohistochemistry of RP1L1 in the Cynomolgus Monkey Retina
Localization of RP1L1 in the rod and cone photoreceptors in the Cynomolgus monkey (*Macaca fascicularis*). Retina labeled with anti-human RP1L1 (red, top); same section labeled with retinal cone specific marker, peanut agglutinin lectin (PNA, green, middle); merged image (bottom). Yellow signal present in cone photoreceptor resulted from combination of the red signal of RP1L1 and the green signal of PNA. Cell nuclei were stained with DAPI (blue). PL, photoreceptor layer; ONL, outer nuclear layer; OPL, outer plexiform layer; INL, inner nuclear layer; IPL, inner plexiform layer; GCL, ganglion cell layer, Scale bars represent 20 μm.

microtubule in the connecting cilia.[17] RP1 contains microtubule-binding domains (amino acids 28–228) of neuronal microtubule-associated protein (MAP) doublecortin (DCX), which is required to maintain axoneme length and stability.[18] The RP1L1 p.Arg45Trp alteration resides in one of the two DCX domains (amino acids 33–113 and 147–228), which is required for interaction with RP1 to assemble and stabilize axonemal microtubules.[8] In primates, both RP1L1 and RP1 proteins may cooperatively function in the rod and cone photoreceptors to perform this task. The mutation in *RP1L1* is likely to dominantly affect the cooperative function with RP1 in rod and cone photoreceptors, given that in a previous publication, the *RP1L1* heterozygous knockout mice were reported to be normal whereas homozygous knockout mice were reported to develop subtle retinal degeneration. Our findings in OMD may shed light for further investigation of patients with cone dystrophy.

In conclusion, we identified *RP1L1* mutations that cause autosomal-dominant OMD, and furthermore, our findings revealed that *RP1L1* plays essential roles in the cone functions in human and that disruption of *RP1L1* function leads to OMD.

Supplemental Data

Supplemental Data include three figures and one table can be found with this article online at http://www.cell.com/AJHG/.

Acknowledgments

This research was supported in part by grants to Takeshi Iwata and Kazushige Tsunoda by the Ministry of Health, Labour, and Welfare of Japan. This work was also supported in part to Shoji Tsuji by KAKENHI (Grant-in-Aid for Scientific Research) on Priority Areas, Applied Genomics, the Global COE Program, and Scientific Research (A) from the Ministry of Education, Culture, Sports, Science and Technology of Japan.

Received: June 29, 2010
Revised: August 10, 2010
Accepted: August 12, 2010
Published online: September 9, 2010

Web Resources

The URLs for data presented herein are as follows:

dbSNP, www.ncbi.nlm.nih.gov/projects/SNP/
SNP HiTLink software, http://www.dynacom.co.jp/u-tokyo.ac.jp/snphitlink/

Accession Numbers

The dbSNP accession numbers for the SNPs reported in this paper are ss252841181 and ss252841182.

References

1. Miyake, Y., Ichikawa, K., Shiose, Y., and Kawase, Y. (1989). Hereditary macular dystrophy without visible fundus abnormality. Am. J. Ophthalmol. *108*, 292–299.

Table 1. Disease-Linked Haplotypes in Families 1 and 2

			Family 1					Family 2	
			Branch 1-1		Branch 1-2				
Probe Set ID	dbSNP rs ID	Position	III-8	IV-9	IV-13	IV-18	IV-21	II-2	III-2
SNP_A-8338925	rs365309	9,064,350	(A)	(A)	A	A	B	A	A
SNP_A-8281994	rs1530483	9,065,671	B	B	B	B	B	B	B
SNP_A-8360926	rs10086673	10,342,727	B	B	(B)	B	B	(A)	A
SNP_A-2082488	rs9329223	10,369,164	A	A	A	A	A	(B)	B
SNP_A-2013182	rs6601491	10,453,427	B	B	B	B	B	(A)	A
RP1L1 p.Arg45Trp	c.133C>T	10,517,989	T	T	T	T	T	T	T
SNP_A-8345504	rs10097570	10,586,268	A	A	A	A	(A)	(B)	B
SNP_A-1790165	rs10111051	10,590,882	A	A	A	A	(A)	(B)	B
SNP_A-8587750	rs2163379	10,769,460	A	A	A	(A)	A	(B)	B
SNP_A-8500791	rs7460507	11,006,485	B	B	B	B	B	A	A
SNP_A-8525908	rs9772321	12,536,010	A	A	A	A	A	A	A
SNP_A-8283296	rs1021087	13,500,502	A	(A)	(A)	A	A	B	B
SNP_A-8441723	rs6987209	14,501,302	B	B	B	B	B	B	B
SNP_A-2044287	rs7818067	15,580,087	A	A	A	A	A	A	A
SNP_A-4273924	rs6992112	16,689,526	A	A	A	A	A	A	(A)
SNP_A-8447659	rs471041	17,707,836	B	B	B	B	B	B	B
SNP_A-8399664	rs2638658	18,713,620	A	(A)	(A)	A	A	(B)	B
SNP_A-4233785	rs2632841	18,716,063	B	B	(B)	B	A	B	B

Disease-linked haplotypes of the two patients (IV-9 and III-8) who are descendants from II-1 (branch 1-1 of family 1), the three patients (IV-13, IV-18, and IV-21) who are descendants from II-7 (branch 1-2 of family 1), and the two patients (II-2 and III-2) from family 2 are shown. Haplotypes are unequivocally determined, except those with brackets that are inferred to minimize the number of recombination events. Disease-linked haplotypes of the two branches of family 1 are the same, confirming that all affected individuals in family 1 share the same haplotype. Recombination events in the family was observed at rs365309 (telomeric boundary) and at rs2632841 (centromereic boundary). When disease haplotypes are compared between families 1 and 2, who share the p.Arg45Trp mutation in *RP1L1* in common, disease-linked haplotypes flanking the *RP1L1* locus are different between these families, suggesting that the p.Arg45Trp mutation originated independently.

2. Miyake, Y., Horiguchi, M., Tomita, N., Kondo, M., Tanikawa, A., Takahashi, H., Suzuki, S., and Terasaki, H. (1996). Occult macular dystrophy. Am. J. Ophthalmol. *122*, 644–653.
3. Wildberger, H., Niemeyer, G., and Junghardt, A. (2003). Multifocal electroretinogram (mfERG) in a family with occult macular dystrophy (OMD). Klin. Monatsbl. Augenheilkd. *220*, 111–115.
4. Piao, C.H., Kondo, M., Tanikawa, A., Terasaki, H., and Miyake, Y. (2000). Multifocal electroretinogram in occult macular dystrophy. Invest. Ophthalmol. Vis. Sci. *41*, 513–517.
5. Brockhurst, R.J., and Sandberg, M.A. (2007). Optical coherence tomography findings in occult macular dystrophy. Am. J. Ophthalmol. *143*, 516–518.
6. Fukuda, Y., Nakahara, Y., Date, H., Takahashi, Y., Goto, J., Miyashita, A., Kuwano, R., Adachi, H., Nakamura, E., and Tsuji, S. (2009). SNP HiTLink: a high-throughput linkage analysis system employing dense SNP data. BMC Bioinfomatics *10*, 121.
7. Gudbjartsson, D.F., Thorvaldsson, T., Kong, A., Gunnarsson, G., and Ingolfsdottir, A. (2005). Allegro version 2. Nat. Genet. *37*, 1015–1016.
8. Yamashita, T., Liu, J., Gao, J., LeNoue, S., Wang, C., Kaminoh, J., Bowne, S.J., Sullivan, L.S., Daiger, S.P., Zhang, K., et al. (2009). Essential and synergistic roles of RP1 and RP1L1 in rod photoreceptor axoneme and retinitis pigmentosa. J. Neurosci. *29*, 9748–9760.
9. Park, S.J., Woo, S.J., Park, K.H., Hwang, J.M., and Chung, H. (2010). Morphologic photoreceptor abnormality in occult macular dystrophy on spectral-domain optical coherence tomography. Invest. Ophthalmol. Vis. Sci. *51*, 3673–3679.
10. Sisk, R.A., Berrocal, A.M., and Lam, B.L. (2010). Loss of foveal cone photoreceptor outer segments in occult macular dystrophy. Ophthalmic Surg Lasers Imaging *41*, 1–3.
11. Conte, I., Lestingi, M., den Hollander, A., Alfano, G., Ziviello, C., Pugliese, M., Circolo, D., Caccioppoli, C., Ciccodicola, A., and Banfi, S. (2003). Identification and characterization of the retinitis pigmentosa 1-like1 gene (RP1L1): a novel candidate for retinal degenerations. Eur. J. Hum. Genet. *11*, 155–162.
12. Bowne, S.J., Daiger, S.P., Malone, K.A., Heckenlively, J.R., Kennan, A., Humphries, P., Hughbanks-Wheaton, D., Birch, D.G., Liu, Q., Pierce, E.A., et al. (2003). Characterization of

Table 2. Summary of RP1L1 Mutations in Families with OMD

ID in Pedigree	Clinical Stage	Sex	Age at Diagnosis	Age at Onset in Estimation	Mutation	Best Corrected Visual Acuity (Right / Left)
1 III3	affected	F	81	50	c.362C>T	1.2 / 0.1
1 III4	affected	F	71	25	c.362C>T	0.4 / 0.5
1 III5	affected	M	74	30	c.362C>T	0.2 / 0.3
1 III8	affected	M	82	20	c.362C>T	0.2 / 0.2
1 IV1	unaffected	F	60	-	c.362C>T	1.2 / 1.2
1 IV9	affected	F	49	unknown	c.362C>T	1.2 / 1.2
1 IV12	affected	F	69	50	c.362C>T	0.1 / 0.07
1 IV13	affected	M	70	20	c.362C>T	0.1 / 0.1
1 IV14	affected	M	66	30	c.362C>T	0.2 / 0.3
1 IV18	affected	F	58	12	c.362C>T	0.1 / 0.1
1 IV21	affected	F	58	47	c.362C>T	0.1 / 0.4
1 V2	affected	M	20	13	c.362C>T	0.3 / 0.3
1 V3	affected	F	19	6	c.362C>T	0.2 / 0.15
2 II2	affected	M	69	unknown	c.362C>T	0.2 / 0.2
2 II4	unaffected	M	58	-	c.362C>T	1.0 / 1.0
2 II5	unaffected	M	55	-	c.362C>T	1.0 / 1.0
2 II8	affected	M	52	unknown	c.362C>T	0.2 / 0.3
2 III1	affected	M	23	23	c.362C>T	0.2 / 0.3
2 III2	affected	M	20	20	c.362C>T	0.3 /0.3
3 II1	affected	F	29	12	c.3107T>C	0.2 / 0.2
3 II3	affected	M	19	13	c.3107T>C	0.2 / 0.3
4 III3	affected	F	52	30	c.362C>T	0.15 / 0.15

Summary of individuals from autosomal OMD families 1–4, in whom p.Arg45Trp or p.Trp960Arg mutations of *RP1L1* were found. Three unaffected individuals at the age of 55–60 were found with the mutation. These individuals suggest a reduced penetrance of the mutation or a possible onset at a later age.

RP1L1, a highly polymorphic paralog of the retinitis pigmentosa 1 (RP1) gene. Mol. Vis. *9*, 129–137.

13. Pierce, E.A., Quinn, T., Meehan, T., McGee, T.L., Berson, E.L., and Dryja, T.P. (1999). Mutations in a gene encoding a new oxygen-regulated photoreceptor protein cause dominant retinitis pigmentosa. Nat. Genet. *22*, 248–254.
14. Sullivan, L.S., Heckenlively, J.R., Bowne, S.J., Zuo, J., Hide, W.A., Gal, A., Denton, M., Inglehearn, C.F., Blanton, S.H., and Daiger, S.P. (1999). Mutations in a novel retina-specific gene cause autosomal dominant retinitis pigmentosa. Nat. Genet. *22*, 255–259.
15. Jacobson, S.G., Cideciyan, A.V., Iannaccone, A., Weleber, R.G., Fishman, G.A., Maguire, A.M., Affatigato, L.M., Bennett, J., Pierce, E.A., Danciger, M., et al. (2000). Disease expression of RP1 mutations causing autosomal dominant retinitis pigmentosa. Invest. Ophthalmol. Vis. Sci. *41*, 1898–1908.
16. Liu, Q., Lyubarsky, A., Skalet, J.H., Pugh, E.N., Jr., and Pierce, E.A. (2003). RP1 is required for the correct stacking of outer segment discs. Invest. Ophthalmol. Vis. Sci. *44*, 4171–4183.
17. Liu, Q., Zuo, J., and Pierce, E.A. (2004). The retinitis pigmentosa 1 protein is a photoreceptor microtubule-associated protein. J. Neurosci. *24*, 6427–6436.
18. Gleeson, J.G., Allen, K.M., Fox, J.W., Lamperti, E.D., Berkovic, S., Scheffer, I., Cooper, E.C., Dobyns, W.B., Minnerath, S.R., Ross, M.E., and Walsh, C.A. (1998). Doublecortin, a brain-specific gene mutated in human X-linked lissencephaly and double cortex syndrome, encodes a putative signaling protein. Cell *92*, 63–72.

Fundus Autofluorescence in Autosomal Dominant Occult Macular Dystrophy

Kaoru Fujinami, MD; Kazushige Tsunoda, MD, PhD; Gen Hanazono, MD; Kei Shinoda, MD, PhD; Hisao Ohde, MD, PhD; Yozo Miyake, MD, PhD

Objective: To characterize fundus autofluorescence (FAF) images of eyes with autosomal dominant occult macular dystrophy (OMD).

Methods: All patients received a comprehensive ophthalmologic examination for diagnosis of OMD. We evaluated the FAF images in 13 eyes of 7 patients with autosomal dominant OMD by confocal scanning laser ophthalmoscopy with excitation at 488 nm and emission more than 500 nm.

Results: The FAF images showed unspecific weak foveal hyperfluorescence in 4 eyes of 2 patients; one showed a thin hyperfluorescence in the temporal fovea bilaterally and the other showed weak hyperfluorescence in the fovea bilaterally. The optical coherence tomographic images showed abnormalities of the photoreceptor inner segment–outer segment line and cone outer segment tip line in all patients. However, 5 patients had normal FAF images regardless of morphological abnormalities of the photoreceptor.

Conclusions: Fundus autofluorescence is a useful method to acquire additional information of photoreceptor/retinal pigment epithelium function in eyes with OMD. Fundus autofluorescence will be also helpful for the differential diagnosis of eyes with OMD vs eyes with other dystrophies that have a distinctive FAF pattern.

Arch Ophthalmol 2011;129(5):597-602

OCCULT MACULAR DYSTROPHY (OMD) is an inherited macular dystrophy with a progressive decrease of visual acuity but with essentially normal fundus and fluorescein angiograms (FAs).[1,2] Patients with OMD have normal full-field electroretinograms (ERGs), but the focal macular ERGs (FMERGs) and multifocal ERGs are abnormal.[1-3] The latter findings are the key for diagnosing OMD. Occult macular dystrophy is inherited as an autosomal dominant trait[1,2,5]; however, patients with sporadic disease have been also reported.[6,7] Optical coherence tomography (OCT) in eyes with OMD showed abnormalities in the foveal structure.[8,9] Recently, a loss of the cone photoreceptor outer segments and defects in the junction of the photoreceptor inner segment–outer segment line were demonstrated in patients with sporadic OMD.[10-12] The most characteristic finding in eyes with OMD that differentiates it from other retinal diseases is the normal-appearing fundus even in the advanced stages. It is conceivable that this normal-appearing fundus has been attributed to well-preserved retinal pigment epithelium (RPE) function.

Lipofuscin is derived from the phagocytosed photoreceptor outer segments and normally accumulates in the RPE.[13-15] Fundus autofluorescence (FAF) recorded with a confocal scanning laser ophthalmoscope can provide information about the distribution of lipofuscin in the RPE of the eyes noninvasively.[16] By being able to detect the lipofuscin mainly at the RPE level, FAF could be a useful method to detect and characterize the lipofuscin distribution in a wide variety of inherited and acquired retinal diseases even when fundus changes are not or have not been clearly shown by routine ophthalmoscopy and FA.[15,17-20]

To our knowledge, the FAF findings in autosomal dominant OMD have not been published, although there are 2 case reports that describe the FAF findings in sporadic OMD.[10,12] However, some of the cases diagnosed with sporadic OMD may have different etiologies because the causative gene of OMD is unknown and eliminating acquired diseases such as age-related macular degeneration is very difficult.

The purpose of this study was to characterize the FAF images in patients with autosomal dominant OMD and to determine whether the FAF images can help in evaluating the photoreceptor turnover of eyes with OMD. To accomplish this, we

Author Affiliations: Laboratory of Visual Physiology, National Institute of Sensory Organs (Drs Fujinami, Tsunoda, Hanazono, Shinoda, Ohde, and Miyake), and Department of Ophthalmology, Kikkoman General Hospital, Noda City (Dr Hanazono), Teikyo University School of Medicine, Tokyo (Dr Shinoda), and Aichi Medical University, Aichi (Dr Miyake), Japan.

Table. Clinical Characteristics of Patients With Autosomal Dominant Occult Macular Dystrophy

Patient No./ Sex/Age	Eye	Years From Onset	BCVA	Refractive Error, D	Central Scotoma	IS-OS Irregularity[a]	ffERG	Amplitude Reduced						FH	Complications
								FMERG			mfERG				
								5°[b]	10°[c]	15°[d]	Ring 1	Ring 2[e]	Ring 3		
1/M/51	OD	3	20/200	−1.68[f]	+	+	Normal	+	+	+	+	+	−	AD	High myopia
	OS	3	20/200	−2.25[f]	+	+	Normal	+	+	+	+	+	−		High myopia
2/F/67	OD	18	20/200	0	+	+	Normal	+	−	−	+	−	−	AD	
	OS	18	20/200	0.63	+	+	Normal	+	+	−	+	+	−		
3/F/80[g]	OD	5	20/100	−1.68[f]	+[h]	+	Normal	+	+	+	+	+	−	AD	Glaucoma, high myopia
	OS	5	20/200	−1.75[f]	...	...	...	...	...	...	...	...	...	...	...
4/F/47	OD	6	20/40	−1.5	+	+	Normal	...	...	...	+	+	−	AD	
	OS	6	20/40	−2	+	+	Normal	...	...	...	+	+	−		
5/M/67	OD	22	20/200	1.25	+	+	Normal	+	+	−	+	+	−	AD	
	OS	22	20/200	2.25	+	+	Normal	+	+	−	+	+	−		
6/F/51	OD	20	20/125	−9	+	+	Normal	+	+	−	+	+	−	AD	High myopia
	OS	20	20/125	−9.38	+	+	Normal	+	+	−	+	+	−		High myopia
7/F/74	OD	3	20/200	−0.13[f]	+	+	Normal	+	+	+	+	+	−	AD	Diabetic retinopathy
	OS	3	20/100	−1.25[f]	+	+	Normal	+	+	+	+	+	−		Diabetic retinopathy

Abbreviations. AD, autosomal dominant; BCVA, best-corrected visual acuity; D, diopters, ERG, electroretinogram; ffERG, full-field ERG, FH, family history; FMERG, focal macular ERG; ellipses, not examined; IOL, intraocular lens, IS-OS, inner segment–outer segment junction, mfERG, multifocal ERG, OCT, optical coherence tomography, OMD, occult macular dystrophy, +, present; −, absent.

[a] All patients except patient 4 underwent Fourier-domain OCT; patient 4 underwent time-domain OCT

[b] In the right eye of patient 2, the abnormality in FMERGs was limited in the 5° diameter.

[c] In the left eye of patient 2 and both eyes of patients 5 and 6, the a- and b-wave amplitudes were severely reduced within the 10° diameter.

[d] The a- and b-wave amplitudes of the FMERGs were severely reduced within the 15° diameter in patients 1, 3, and 7

[e] The mfERGs were reduced within ring 2 in both eyes of patient 4

[f] Patients 1, 3, and 7 had pseudophakic eyes (IOL)

[g] Only the right eye of patient 3 was examined because the left eye had an idiopathic epiretinal membrane

[h] In Patient 3, visual field testing detected glaucomatous damage in addition to OMD.

investigated the FAF images of 13 eyes in 7 patients who had been diagnosed with autosomal dominant OMD.

METHODS

We studied 13 eyes of 7 patients diagnosed with OMD. All of the patients had a family history of OMD and were diagnosed with autosomal dominant OMD. All of the patients were being studied at the National Institute of Sensory Organs, Tokyo, Japan. An informed consent was obtained after a full explanation of the procedures. All studies were conducted in accordance with the Declaration of Helsinki.

There were 2 men and 5 women whose ages ranged from 47 to 80 years (mean, 51.0 years). One eye was excluded because it had an idiopathic epiretinal membrane. The ophthalmological examinations included best-corrected visual acuity measurement, refraction, slitlamp biomicroscopy, ophthalmoscopy, fundus photography, perimetry, OCT, FA, FAF, full-field ERGs, and focal ERGs. Patients 2 and 5 chose not to receive FA. The FMERGs were recorded from 11 eyes of 6 patients and multifocal ERGs, from 13 eyes of 7 patients.

The visual fields were determined by Goldmann perimetry or the Humphrey Visual Field Analyzer (model 750, Carl Zeiss Meditec, Inc, Dublin, California). The Swedish interactive threshold algorithm standard strategy was used with program 30-2 of the Humphrey Visual Field Analyzer.

The OCT images were recorded using a Fourier-domain OCT (HD-OCT; Carl Zeiss Meditec) in all patients except patient 4, who was examined with a time-domain OCT (TD-OCT, Carl Zeiss Meditec).

Full-field ERGs were recorded using an extended testing protocol incorporating International Society for Clinical Electrophysiology of Vision standards.[31] The ERGs were used to assess the retinal function under both scotopic and photopic states.

The FMERGs were recorded with a commercially available FMERG system (ER80, Kowa Company, Tokyo, Japan, and Mayo Company, Nagoya, Japan) using a bipolar contact lens electrode (Burian-Allen ERG Electrode; Hansen Ophthalmic Laboratories, Iowa City, Iowa). The stimulus and background lights were integrated in the infrared fundus camera.[32-34] The size of the stimulus spot was varied from 5°, 10°, and 15° in diameter and was placed on the macula by observing the infrared image on a monitor. The white stimulus and background illumination were generated by light-emitting diodes and had maximal spectral emissions of 440 to 460 nm and 550 to 580 nm, respectively. The luminances of the stimuli and background were 115.7 cd/m^2 and 8.0 cd/m^2. The duration of the stimulation was 100 milliseconds. The responses were amplified and filtered by digital band-pass filters from 5 to 200 Hz (Neuropack μ, MEB 9102, Nihonkoden, Tokyo). Five hundred responses were summed with a stimulus frequency of 5 Hz.

The multifocal ERGs were recorded with the Visual Evoked Response Imaging System (EDI, San Mateo, California) using a Burian-Allen ERG electrode. The visual stimuli consisted of 61 hexagonal elements with an overall subtense of approximately 60°. The luminance of each hexagon was independently modulated between black (3.5 cd/m^2) and white (138.0 cd/m^2) according to a binary m-sequence at 75 Hz. The surround luminance was set at 70.8 cd/m^2.[35,36]

The FAF images were recorded with a confocal scanning laser ophthalmoscope (model HRA/HRA2; Heidelberg Engineering, Dossenheim, Germany) after the pupil was dilated, and the recordings followed the protocol of Smith et al.[37] This instrument uses a blue laser light at 488 nm for illumination and a barrier filter at 500 nm to limit the fluorescence to the autofluorescent struc-

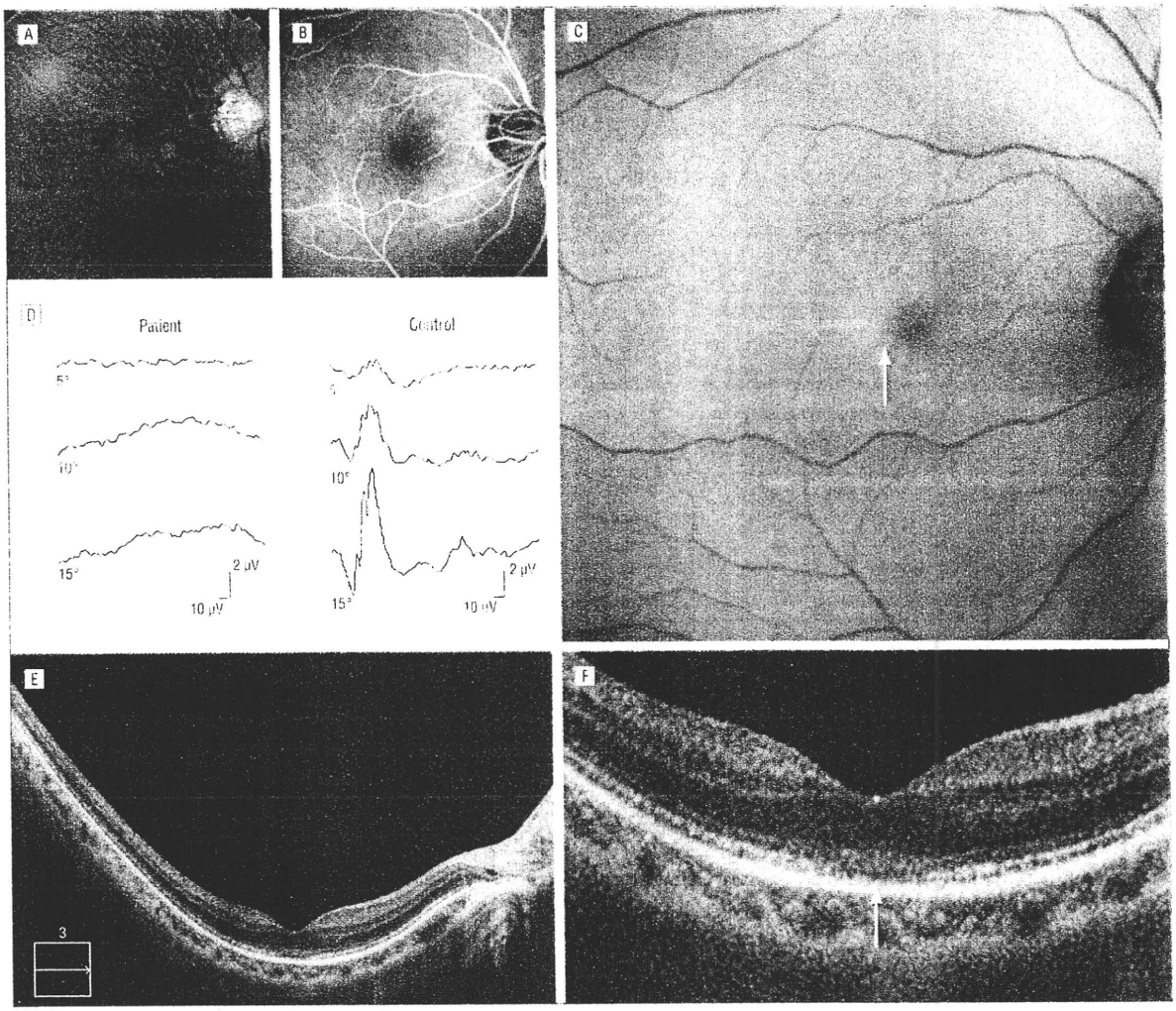

Figure 1. Patient 1 examination results. A, Fundus photograph. B, Fluorescein angiogram. C, Fundus autofluorescence image showing thin hyperfluorescence in the temporal fovea (arrow). D, Focal macular electroretinograms (ERGs). The ERG of a normal control is shown to the right of the patient's ERG for comparison. E, Optical coherence tomographic image of the right eye. F, Extended optical coherence tomographic image of the fovea of the right eye.

tures. The radiant power through the pupil was 180 μW, which gave a retinal irradiance of 227 μW/cm² for a field of 30° square. The acquisition time was 15 to 50 seconds. The scanned FAF images were recorded as JPEG files that were 512 × 512 pixels. The gain setting was 94% and each image was the average of 9 raw scans.

RESULTS

The diagnosis of OMD was made by the following findings: bilateral involvement, gradually decreasing visual acuity, normal ophthalmoscopic findings, normal FA, normal scotopic and photopic full-field ERGs, and absence or decrease of the amplitude of the FMERGs. All of our patients had the inheritance pattern of autosomal dominant as expected for OMD. Because FA was not performed in patients 2 and 5, we were careful in diagnosis and used the information of the other families who had already been diagnosed with OMD.

The clinical characteristics of the 7 patients are shown in the **Table**. The mean interval from the onset of the subjective visual decrease to the time of examination was 11 years with a range from 3 to 22 years. The best-corrected visual acuities ranged from 20/200 to 20/40. The spherical equivalent refractive error ranged from −9.38 to +2.25 diopters. Five eyes were pseudophakic. All patients had a central scotoma except for patient 3 who had both a central scotoma and a superior nasal visual field defect due to glaucoma. The FMERGs and multifocal ERGs were reduced in all patients within the 5° to 15° central region (Table). The OCT images showed an irregularity of the inner segment–outer segment line and loss of the cone outer segment tip line at the fovea in all patients.

Of 13 eyes of 7 patients, 4 eyes of 2 patients showed FAF abnormalities at the fovea and 9 eyes of 5 patients showed no abnormalities in the FAF images. The 4 eyes had hyperfluorescent lesions and none of the eyes had hypofluorescent lesions.

The results of our examination on patient 1, a typical case of OMD, are shown in **Figure 1**. The patient was a

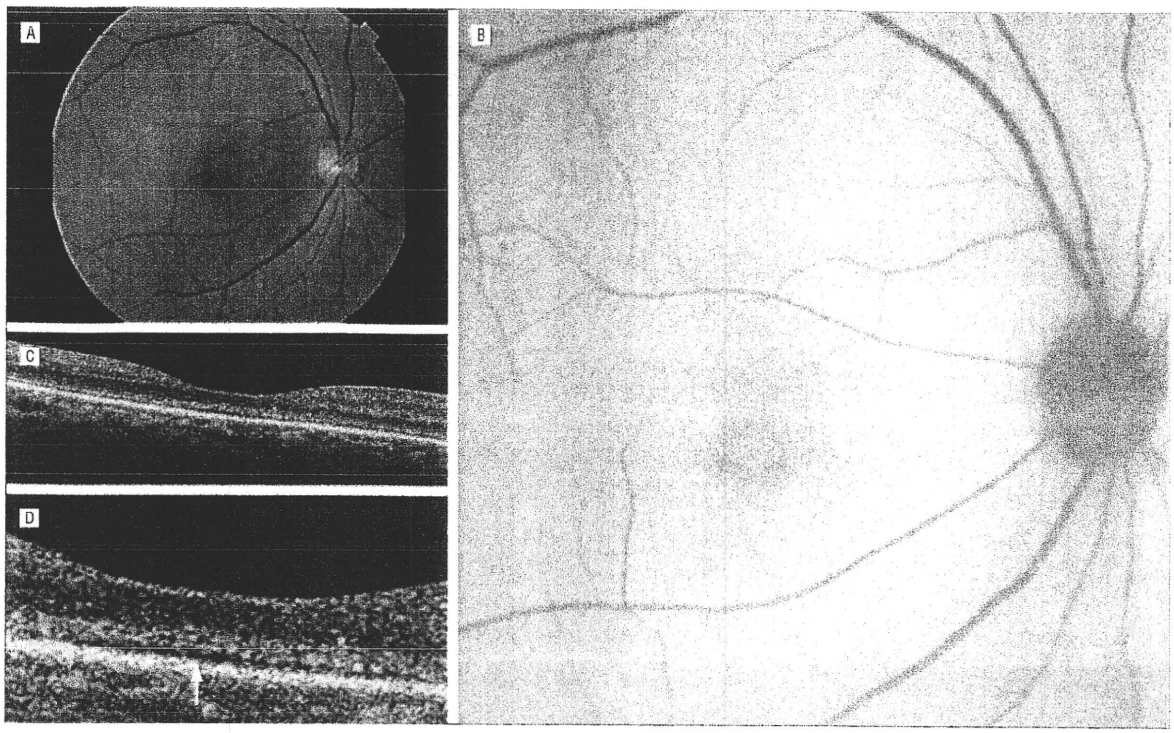

Figure 2. Patient 2 examination results. A, Fundus photograph. B, Fundus autofluorescence image showing weak hyperfluorescence in the central fovea. C, Optical coherence tomographic image of the right eye. D, Extended optical coherence tomographic image of the fovea of the right eye.

51-year-old man with a best-corrected visual acuity of 20/200 in both eyes. He complained of bilateral visual decrease and a blind spot in the central field for 3 years. He had an autosomal dominant inheritance pattern. His mother, patient 3, had the same symptoms. Ophthalmoscopy (Figure 1A) and FA (Figure 1B) showed that his macula was normal. Static perimetry detected a central scotoma bilaterally. Although all components of the full-field ERGs were slightly reduced because of the high myopia, they were not reduced enough to alter the diagnosis of OMD. The a- and b-waves of the FMERGs were abolished in amplitudes with prolonged implicit times in the responses elicited by 5°, 10°, and 15° stimuli (Figure 1D). The OCT images showed that the inner segment-outer segment line was disrupted at the fovea and the cone outer segment tip line was not present in the entire macular region (Figure 1E and F [arrow]). The FAF images had a thin hyperfluorescence in the temporal fovea of the right eye (Figure 1C [arrow]). The hyperfluorescence was annular; however, the border in the nasal area was not clear. All examination findings were bilaterally symmetrical. The FAF abnormalities were restricted to the fovea, sparing the foveola, while morphological abnormalities were present in the entire macula.

The results from patient 2 are shown in **Figure 2**. Although the macula was normal, the FAF image showed weak hyperautofluorescence in the central fovea (Figure 2A and B). The OCT images also showed an irregularity of the inner segment–outer segment line and the loss of the cone outer segment tip line at the fovea (Figure 2C and D [arrow]). The results were bilaterally symmetrical.

The FAF images of patients 3, 4, and 5 and the OCT images of patient 3 are shown in **Figure 3**. The FAF images appeared normal, although the OCT images showed the same abnormality at the fovea as in patients 1 and 2 (Figure 3C [arrow]). There was a shadow of medial opacity in patient 3 (Figure 3).

COMMENT

We investigated the FAF images associated with photoreceptor outer segment turnover or RPE dysfunction in eyes with autosomal dominant OMD. Our results showed that FAF images had weak hyperautofluorescent changes at the fovea in 4 eyes of 2 patients and no abnormalities in 9 eyes of 5 patients. In general, the FAF images in OMD were not severely abnormal, which indicates that the FAF results can be used in the differential diagnosis of OMD from other macular dystrophies. It was very difficult to quantify the influence of aging on the FAF findings because (1) the observation period of each patient was very short and (2) the duration between the onset and the time of examination could not be determined accurately because OMD is a slowly progressive disease and the time of onset based on patients' concern is not reliable. In addition, we could not completely eliminate the existence of macular pigments blocking the 488-nm autofluorescence, which could modify the autofluorescence from lipofuscin in the fovea.[38] Estimation of the density of the macular pigment could be helpful for a more precise degree of autofluorescence derived from fluorophore in RPE.

Fundus autofluorescence was also valuable in assessing the condition of photoreceptor outer segment turn-

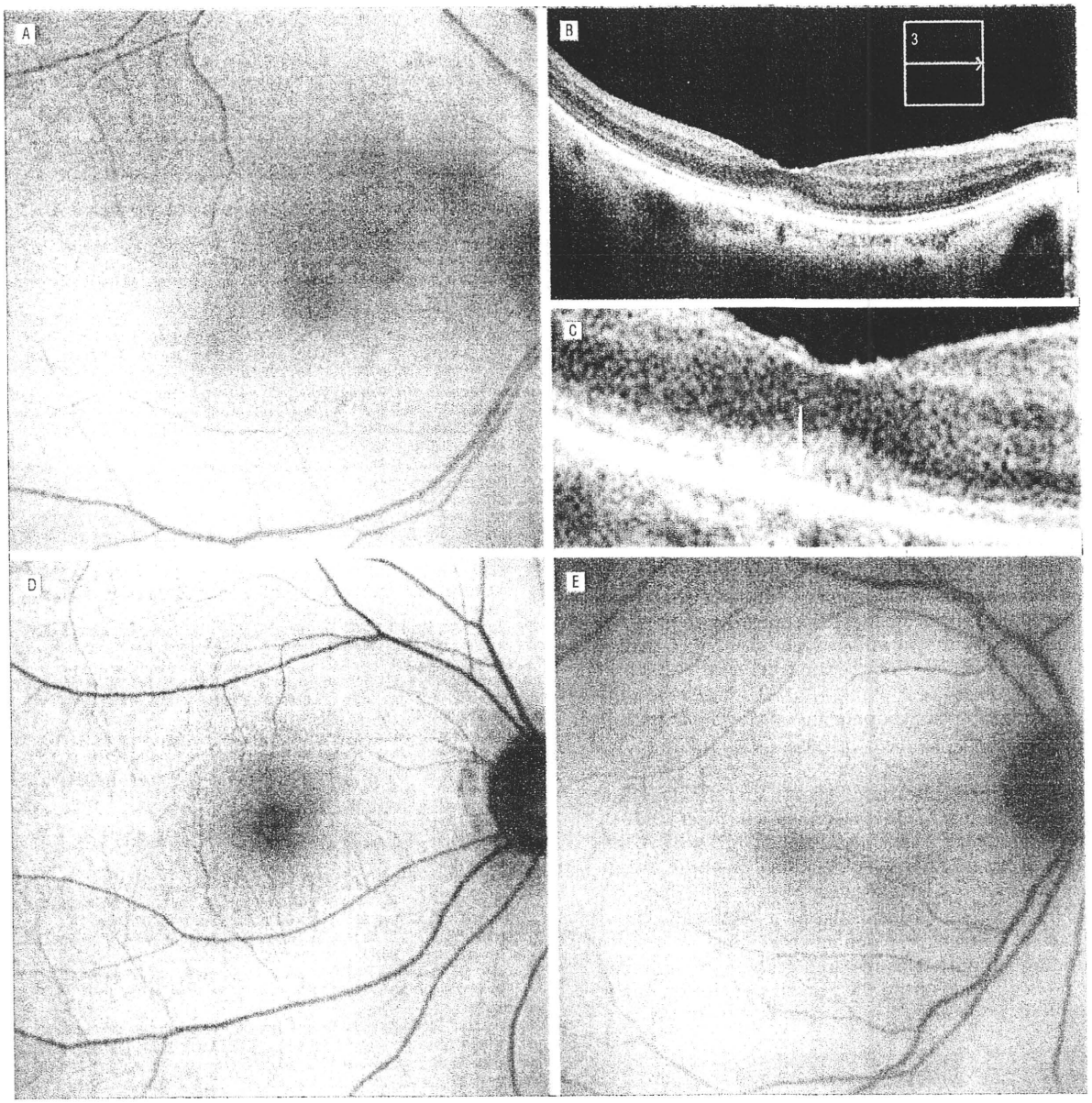

Figure 3. Results for patients 3, 4, and 5. A, Fundus autofluorescence (FAF) image of patient 3. B, Optical coherence tomographic image of patient 3. C, Extended optical coherence tomographic image of the fovea of patient 3. The arrow shows the same abnormality as in patients 1 and 2. D, The FAF image of patient 4. E, The FAF image of patient 5. The FAF images show no abnormalities in the fovea.

over in OMD. Weak hyperautofluorescent changes in the 2 patients implied an increased photoreceptor outer segment turnover, which could have been caused by photoreceptor death. On the other hand, in 5 patients, the functional and morphological damage in the photoreceptor was shown by the reduced FMERG amplitudes and OCT, even though FAF abnormalities were not identified. This inconsistency suggests that the degree of progression in the photoreceptor damage was so gradual that the FAF images did not manifest the abnormalities in the photoreceptor outer segment turnover, such as a hyperautofluorescent lesion. Fundus autofluorescence could give us information regarding the degree of progression in OMD.

In the 4 eyes with abnormal FAF, OCT demonstrated abnormalities over the entire macula area, although the FAF abnormalities were restricted to the fovea. The localized hyperfluorescence in the FAF images may be because the photoreceptor outer segment turnover was not uniform at a particular stage of the disease progress. Hyperautofluorescence in the FAF images is prominent when the disease is progressing, such as in retinitis pigmentosa and geographic atrophy.[39] Fundus autofluorescence measurements when the symptoms first appear might reveal some initial changes in the outer segment metabolism in OMD.

None of our patients with OMD showed decreased or absent FAF, which reflects RPE loss or atrophy. In ad-

dition, the appearance of the RPE in the OCT is always normal in the entire macular region, although damage of the photoreceptors was detected. This implies that the primary lesion of OMD is of the cone photoreceptors and the RPE is not damaged fatally even in the late stages.

Autosomal dominant OMD is considered to be a central cone dystrophy.[2] It is well known that the FAF images of eyes with other dystrophies show distinct patterns of FAF abnormalities. Retinitis pigmentosa shows a ring of high-density fluorescence,[15,17,36] and parafoveal rings have also been observed in Leber congenital amaurosis,[15,33] Best disease,[15,27] X-linked retinoschisis,[15,28] and cone-rod dystrophy.[15,24] In Stargardt disease, RPE atrophy leads to a characteristic hypofluorescent appearance and flecks show distinct abnormalities in the FAF.[26] Pattern dystrophy shows hypofluorescent lesions or patchy multiple hyperfluorescent/hypofluorescent lesions.[30]

The FAF images of OMD did not have any pathognomonic abnormalities, unlike other dystrophies. Although patient 1 had a disconnected ringlike hyperautofluorescence at the fovea, it was definitely different from the shapes of other retinal dystrophies. This was probably because autosomal dominant OMD has distinctly different clinical characteristics from other dystrophies. We do not have sufficient information on the FAF pattern in sporadic cases of OMD[10,12] and whether they have the same features as our patients. The FAF images allow differentiating autosomal dominant OMD from other retinal dystrophies that have distinctive FAF findings.

Submitted for Publication: May 13, 2011; final revision received September 7, 2010; accepted September 20, 2010.
Correspondence: Kazushige Tsunoda, MD, PhD, Laboratory of Visual Physiology, National Institute of Sensory Organs, 2-5-1, Higashigaoka, Meguro-ku, Tokyo 152-8902, Japan (tsunodakazushige@kankakuki.go.jp).
Financial Disclosure: None reported.
Funding/Support: This research was supported in part by research grants from the Ministry of Health, Labor, and Welfare (Japan).

REFERENCES

1 Miyake Y, Ichikawa K, Shiose Y, Kawase Y. Hereditary macular dystrophy without visible fundus abnormality. *Am J Ophthalmol.* 1986;102(3):292-299.
2 Miyake Y, Horiguchi M, Tomita N, et al. Occult macular dystrophy. *Am J Ophthalmol.* 1996;122(5):644-653.
3 Piao CH, Kondo M, Tanikawa A, Terasaki H, Miyake Y. Multifocal electroretinogram in occult macular dystrophy. *Invest Ophthalmol Vis Sci.* 2000;41(2):513-517.
4 Fujii S, Escaño MF, Ishibashi K, Matsuo H, Yamamoto M. Multifocal electroretinography in patients with occult macular dystrophy. *Br J Ophthalmol.* 1999;83(7):879-880.
5 Wildberger H, Niemeyer G, Junghardt A. Multifocal electroretinogram (mfERG) in a family with occult macular dystrophy (OMD). *Klin Monbl Augenheilkd.* 2003;220(3):111-115.
6 Matthews GP, Sandberg MA, Berson EL. Foveal cone electroretinograms in patients with central visual loss of unexplained etiology. *Arch Ophthalmol.* 1992;110(11):1568-1570.
7 Lyons JS. Non-familial occult macular dystrophy. *Doc Ophthalmol.* 2005;111(1):49-56.
8 Kondo M, Ito Y, Ueno S, Piao CH, Terasaki H, Miyake Y. Foveal thickness in occult macular dystrophy. *Am J Ophthalmol.* 2003;135(5):725-728.
9 Brockhurst RJ, Sandberg MA. Optical coherence tomography findings in occult macular dystrophy. *Am J Ophthalmol.* 2007;143(3):516-518.
10 Koizumi H, Maguire JI, Spaide RF. Spectral domain optical coherence tomographic findings of occult macular dystrophy. *Ophthalmic Surg Lasers Imaging.* 2009;40(2):174-176.
11 Park SJ, Woo SJ, Park KH, Hwang JM, Chung H. Morphologic photoreceptor abnormality in occult macular dystrophy on spectral-domain optical coherence tomography. *Invest Ophthalmol Vis Sci.* 2010;51(7):3673-3679.
12 Sisk RA, Berrocal AM, Lam BL. Loss of foveal cone photoreceptor outer segments in occult macular dystrophy. *Ophthalmic Surg Lasers Imaging.* 2010;1-3.
13 Wing GL, Blanchard GC, Weiter JJ. The topography and age relationship of lipofuscin concentration in the retinal pigment epithelium. *Invest Ophthalmol Vis Sci.* 1978;17(7):601-607.
14 Kennedy CJ, Rakoczy PE, Constable IJ. Lipofuscin of the retinal pigment epithelium: a review. *Eye (Lond).* 1995;9(pt 6):763-771.
15 Robson AG, Michaelides M, Saihan Z, et al. Functional characteristics of patients with retinal dystrophy that manifest abnormal parafoveal annuli of high density fundus autofluorescence: a review and update. *Doc Ophthalmol.* 2008;116(2):79-89.
16 von Rückmann A, Fitzke FW, Bird AC. Distribution of fundus autofluorescence with a scanning laser ophthalmoscope. *Br J Ophthalmol.* 1995;79(5):407-412.
17 von Rückmann A, Fitzke FW, Bird AC. Distribution of pigment epithelium autofluorescence in retinal disease state recorded in vivo and its change over time. *Graefes Arch Clin Exp Ophthalmol.* 1999;237(1):1-9.
18 Lois N, Holder GE, Fitzke FW, Plant C, Bird AC. Intrafamilial variation of phenotype in Stargardt macular dystrophy-fundus flavimaculatus. *Invest Ophthalmol Vis Sci.* 1999;40(11):2668-2675.
19 Lois N, Halfyard AS, Bird AC, Fitzke FW. Quantitative evaluation of fundus autofluorescence imaged "in vivo" in eyes with retinal disease. *Br J Ophthalmol.* 2000;84(7):741-745.
20 Lois N, Holder GE, Bunce C, Fitzke FW, Bird AC. Phenotypic subtypes of Stargardt macular dystrophy-fundus flavimaculatus. *Arch Ophthalmol.* 2001;119(3):359-369.
21 Holder GE, Robson AG, Hogg CR, Kurz-Levin M, Lois N, Bird AC. Pattern ERG clinical overview, and some observations on associated fundus autofluorescence imaging in inherited maculopathy. *Doc Ophthalmol.* 2003;106(1):17-23.
22 Robson AG, Egan C, Holder GE, Bird AC, Fitzke FW. Comparing rod and cone function with fundus autofluorescence images in retinitis pigmentosa. *Adv Exp Med Biol.* 2003;533:41-47.
23 Scholl HP, Chong NH, Robson AG, Holder GE, Moore AT, Bird AC. Fundus autofluorescence in patients with Leber congenital amaurosis. *Invest Ophthalmol Vis Sci.* 2004;45(8):2747-2752.
24 Michaelides M, Holder GE, Hunt DM, Fitzke FW, Bird AC, Moore AT. A detailed study of the phenotype of an autosomal dominant cone-rod dystrophy (CORD7) associated with mutation in the gene for RIM1. *Br J Ophthalmol.* 2005;89(2):198-206.
25 Bindewald A, Schmitz-Valckenberg S, Jorzik JJ, et al. Classification of abnormal fundus autofluorescence patterns in the junctional zone of geographic atrophy in patients with age related macular degeneration. *Br J Ophthalmol.* 2005;89(7):874-878.
26 Robson AG, Saihan Z, Jenkins SA, et al. Functional characterisation and serial imaging of abnormal fundus autofluorescence in patients with retinitis pigmentosa and normal visual acuity. *Br J Ophthalmol.* 2006;90(4):472-479.
27 Spaide RF, Noble K, Morgan A, Freund KB. Vitelliform macular dystrophy. *Ophthalmology.* 2006;113(8):1392-1400.
28 Tsang SH, Vaclavik V, Bird AC, Robson AG, Holder GE. Novel phenotypic and genotypic findings in X-linked retinoschisis. *Arch Ophthalmol.* 2007;125(2):259-267.
29. Poloschek CM, Hansen LL, Bach M. Annular fundus autofluorescence abnormality in a case of macular dystrophy. *Doc Ophthalmol.* 2008;116(2):91-95.
30 Renner AB, Fiebig BS, Weber BH, et al. Phenotypic variability and long-term follow-up of patients with known and novel PRPH2/RDS gene mutations. *Am J Ophthalmol.* 2009;147(3):518-530.
31 Marmor MF, Holder GE, Seeliger MW, Yamamoto S. International Society for Clinical Electrophysiology of Vision. Standard for clinical electroretinography (2004 update). *Doc Ophthalmol.* 2004;108(2):107-114.
32 Miyake Y. Focal macular electroretinography. *Nagoya J Med Sci.* 1998;61(3-4):79-84.
33 Miyake Y, Shiroyama N, Horiguchi M, Ota I. Asymmetry of focal ERG in human macular region. *Invest Ophthalmol Vis Sci.* 1989;30(8):1743-1749.
34 Miyake Y. Macular oscillatory potentials in humans: macular OPs. *Doc Ophthalmol.* 1990;75(2):111-124.
35 Sutter EE, Tran D. The field topography of ERG components in man, I: the photopic luminance response. *Vision Res.* 1992;32(3):433-446.
36 Bearse MA Jr, Sutter EE. Imaging localized retinal dysfunction with the multifocal electroretinogram. *J Opt Soc Am A Opt Image Sci Vis.* 1996;13(3):634-640.
37 Smith RT, Komarek JP, Chan J, Nagasaki T, Sparrow JR, Langton K. Autofluorescence characteristics of normal foveas and reconstruction of foveal autofluorescence from limited data subsets. *Invest Ophthalmol Vis Sci.* 2005;46(8):2940-2946.
38 Delori FC. Autofluorescence method to measure macular pigment optical densities fluorometry and autofluorescence imaging. *Arch Biochem Biophys.* 2004;430(2):156-162.
39 Holz FG, Bellman C, Staudt S, Schütt F, Völcker HE. Fundus autofluorescence and development of geographic atrophy in age-related macular degeneration. *Invest Ophthalmol Vis Sci.* 2001;42(5):1051-1056.

Clinical Ophthalmology Dove

ORIGINAL RESEARCH

Pattern-reversal visual-evoked potential in patients with occult macular dystrophy

Gen Hanazono[1,2]
Hisao Ohde[2,3]
Kei Shinoda[1,4]
Kazushige Tsunoda[1,2]
Kazuo Tsubota[2]
Yozo Miyake[1,5]

[1]Department of Ophthalmology, National Institute of Sensory Organs, Tokyo, Japan; [2]Department of Ophthalmology, Keio University School of Medicine, Tokyo, Japan; [3]Kamoshita Eye Clinic, Tokyo, Japan; [4]Department of Ophthalmology, Teikyo University School of Medicine, Tokyo, Japan; [5]Aichi Medical School, Aichi, Japan

Purpose: Occult macular dystrophy (OMD) is a hereditary retinal disease characterized by a normal fundus, normal full-field electroretinograms (ERGs), progressive decrease of visual acuity, and abnormal focal macular ERGs. The purpose of this study was to report pattern-reversal visual-evoked potential (pVEPs) findings in OMD patients.

Patients and method: The pVEPs recorded from four patients with OMD (aged 42–61 years; 2 men and 2 women) were reviewed. The visual acuities ranged from 20/200 to 20/30. The amplitudes of the N-75 and P-100 (P2 amplitude) and the latency of the N-75 components (N1 latency) were analyzed.

Results: The mean (±SD) P2 amplitude was 2.7 ± 1.9 μV for the 5′, 4.8 ± 2.9 μV for the 10′, 3.2 ± 2.1 μV for the 20′, and 4.4 ± 3.5 μV for the 40′ checkerboard stimuli. The N1 latency was 122.2 ± 6.4 ms for the 5′, 105.0 ± 11.5 ms for the 10′, 97.7 ± 10.0 ms for the 20′, and 91.0 ± 13.7 ms for the 40′ checkerboard stimuli. The mean P2 amplitude was reduced and the N1 latency was delayed in comparison with the laboratory standard for the Keio University Hospital.

Conclusions: The delayed latency and reduced amplitude suggest a major contribution of the central cone pathway to the pVEPs.

Keywords: occult macular dystrophy, visual-evoked potential, electroretinogram

Introduction

Occult macular dystrophy (OMD) is a hereditary macular dystrophy characterized by a progressive decrease of the visual acuity, normal fundus, and normal fluorescein angiograms.[1,2] The hereditary form is an autosomal dominant trait, and recently the response gene was identified with mutation in *RP1L1*.[3]

The cone and rod components of the full-field electroretinograms (ERGs) are normal, but the focal macular ERGs are reduced. A reduction of the visual acuity without visible fundus abnormalities, and the presence of a central scotoma and/or reduced central fusion flicker frequency[4] are often seen, and the patients can be misdiagnosed with amblyopia, optic nerve disease, or a nonorganic visual disorder.[4] Only limited information is available on the visual-evoked potentials (VEPs) in patients with OMD.[5] How the VEPs are affected in this disease with central cone dysfunction has not been fully determined. Thus, the purpose of this study was to evaluate the pattern-reversal VEPs (pVEPs) in patients with OMD.

Correspondence: Kei Shinoda
Department of Ophthalmology, Teikyo University School of Medicine, 2-11-1 Kaga, Itabashi-ku, Tokyo 173-8606, Japan
Tel +81 3 3964 1225
Fax +81 3 3964 1402
Email shinodak@med.teikyo-u.ac.jp

Subjects and methods

Subjects

Four patients diagnosed with OMD at the Keio University Hospital between 2000 and 2002 were studied; two were men and two were women aged 42, 49, 60, and 69 years, respectively (Table 1).

Stimulus and recording of pattern-reversal VEPs

The visual stimulus was a black-and-white pattern checkerboard generated on a CRT (cathode ray tube) monitor (20-inch, high-resolution display; Ikegami Tsushinki Co, Ltd, Tokyo, Japan). The mean luminance was kept at 109.5 cd/m^2, and each check was either white (154 cd/m^2) or black (65 cd/m^2) with a 40.6% contrast. Four check sizes were used: 5, 10, 20, and 40 min of arc at an observation distance of 150 cm. The amplitude of N-75 and P-100 (P2 amplitude) and the latency of the N-75 (N1 latency) were analyzed.

Patients were preadapted to the room lighting, and all recordings were performed under dim room lights with an illumination of about 50 cd/m^2. A small black fixation point was present in the center of the stimulus display, and the subjects were instructed to fixate the point or the center of the screen and to try not to blink. The subjects wore their best refractive correction, and all recordings were monocular.

The recording electrode was placed 2.0 cm superior to the inion, and the reference electrode was placed on one earlobe. The ground electrode was placed on the other earlobe.

Signals were amplified 50,000 times with an amplifier (VC-11; Nihon Kohden, Tokyo, Japan) and filtered with a band-pass filter from 0.5 to 30 Hz. Sixty-four responses were averaged.

Normative data were collected from 40 age-matched patients who did not have any ocular diseases except for refractive errors (age range 40–67 years; average 53.1 ± 8.41 years).

All of the procedures conformed to the guidelines of the Declaration of Helsinki, and an informed consent was obtained from all subjects after an explanation of the purpose and the procedures to be used in the experiments.

Results

Patients were diagnosed with OMD by the following findings in both eyes: progressive decrease in the visual acuity, normal fundus, normal fluorescein angiograms, central scotoma in Goldman perimetry, normal cone and rod components of the full-field ERGs, and abnormal focal macular or multifocal ERGs (mfERGs). Their visual acuities ranged from 20/200 to 20/30. None had a history of ophthalmological abnormalities, such as glaucoma or diabetic retinopathy that could affect the visual function especially the pVEPs.

All cases had at least one individual in their pedigree who was also diagnosed with OMD. Case 4 was a second cousin of case 2 (Table 1). The interval between the onset of the decreased visual acuity and diagnosis at our clinic was 1–25 years. Three of the cases were genetically diagnosed with OMD.

VEP results

A plot of the P2 amplitudes as a function of pattern check size in the four patients with OMD is shown in Figure 1A. In three of the cases, the amplitudes of P2 were smaller

Table 1 Clinical characteristics of the patients and the result of the examinations

Patient	Age and gender	Family history	BCVA		Visual field	Fundus appearance	Fluorescein angiography	Full field ERG	Multifocal ERG	Genetic diagnosis
			OD	OS						
1	42, Female	+	20/200	20/200	Central scotoma	Normal	Normal	Normal	Decreased amplitude in fovea	Mutation in *RP1L1*
2	61, Female	+	20/200	20/200	Central scotoma	Normal	Normal	Normal	Decreased amplitude in fovea	Mutation in *RP1L1*
3	60, Male	+	20/60	20/200	Central scotoma	Normal	Normal	Normal	Decreased amplitude in fovea	Mutation in *RP1L1*
4	49, Male	+	20/30	20/30	Central scotoma	Normal	Normal	Normal	Decreased amplitude in fovea	Not examined

Notes: Case 4 is a second cousin of case 2. Focal macular electroretinograms (ERGs) were recorded in patients 1. Multifocal ERGs were recorded from all the patients.
Abbreviations: BCVA, best-corrected visual acuity; OD, right eye; OS, left eye.

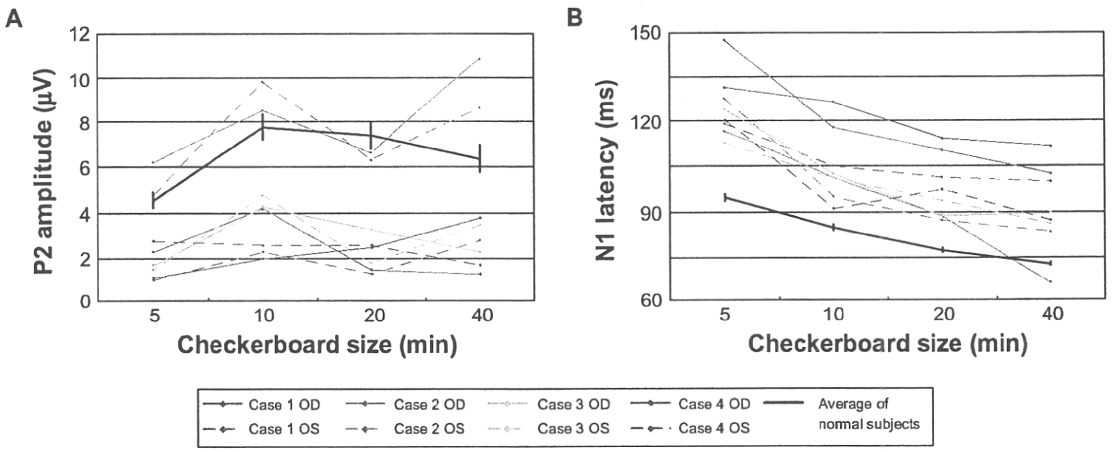

Figure 1 Plot of the A) P2 amplitude and B) N1 latency as a function of the size of the checks of the stimulus for the four patients. The average and the standard error of the means of normal subjects are plotted as the black line. The N1 latency was delayed in all eyes, while the P2 amplitude was reduced in all eyes except both eyes in case 2.

than that of the normal controls. In the second case (case 2), the P2 amplitudes overlapped the amplitudes of the normal controls.

The latencies of the N-75 component from all of the patients were longer than those of normal subjects (Figure 1B).

Case reports

All four cases share typical OMD features, and definitive diagnosis was made genetically in the three of four cases. We present case 1 as the representative data.

Case 1

Case 1 was a 42-year-old woman who stated that her visual acuity has been reduced in both eyes for 10 years. Several ophthalmologists, psychiatrists, and physicians in other clinics failed to diagnose her condition, and she was referred to Keio University Hospital for further examination. Her sister and cousin had similar symptoms – bilateral progressive decrease of vision – and were diagnosed with OMD at other hospitals. Her corrected visual acuity was 20/200 in both eyes. Funduscopy and fluorescein angiography were normal (Figure 2). Goldman perimetry showed a central scotoma of 5° in both eyes (Figure 3). The central fusion flicker frequency was 28.6 Hz in the right eye and 29.6 Hz in the left eye (48.2 ± 5.3 Hz: mean ± SD as normal range in our laboratory). Her right eye had normal color vision, and her left eye had mild atypical dyschromatopsia.

The scotopic, bright-flash, photopic, and 30-Hz flicker full-field ERGs were normal (Figure 4). However, the mfERGs in the central areas were reduced (Figure 3). The focal macular ERGs recorded at another clinic were clearly reduced in both eyes (Figure 5). A diagnosis of OMD was made.

The P2 amplitude was 2.3 μV for the 5′, 4.2 μV for the 10′, 1.5 μV for the 20′, and 1.3 μV for the 40′ checkerboard stimuli of the right eye (Figure 6). For the same stimuli for the left eye, the P2 amplitudes were 1.0, 2.3, 1.3, and 2.8 μV, respectively. The N1 latency was 147.5 ms for the 5′, 117.5 ms for the 10′, 110.0 ms for the 20′, and 102.5 ms for the 40′ checkerboard stimuli in right eye (Figure 1B). For the left eye and the same stimuli, the N2 latencies were 118.8, 105.0, 101.3, and 100.0 ms, respectively. The average P2 amplitude was reduced, and the N1 latency was delayed in comparison to our laboratory standard values (Figure 1).

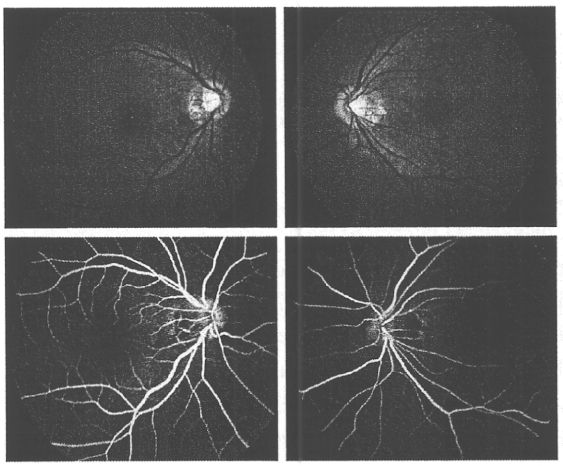

Figure 2 Fundus photograph (above) and fluorescein angiography (below) of case 1 showing no abnormal findings.